TMS ICME

MANUFACTURING

DESIGN MATERIALS

Proceedings of the 2nd World Congress on Integrated Computational Materials Engineering (ICME)

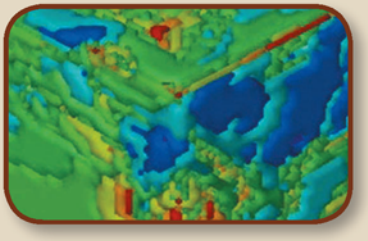

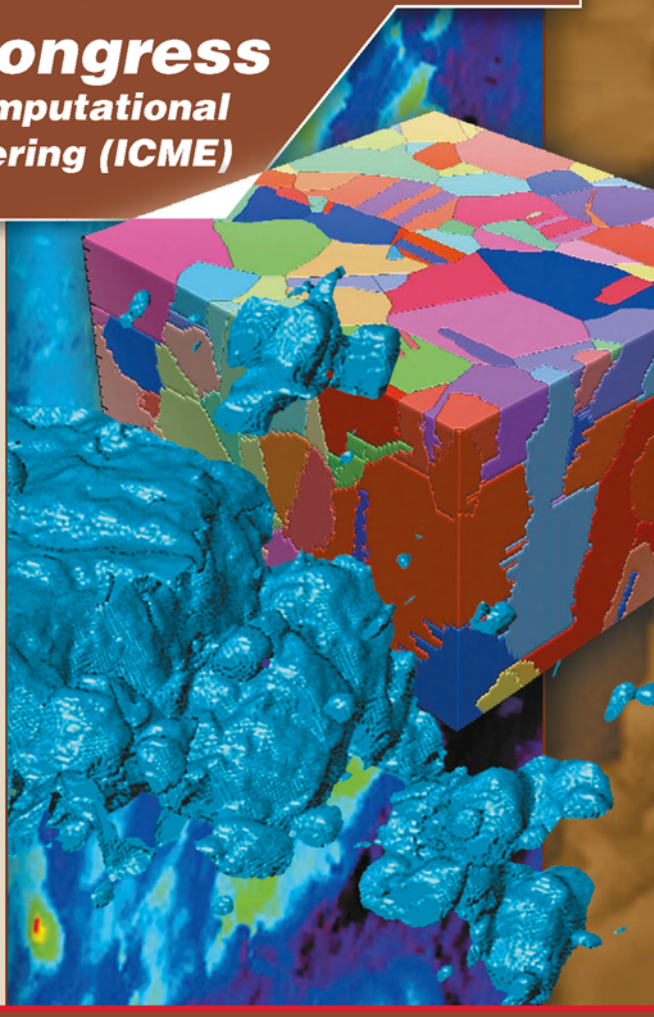

Edited by

Mei Li
Carelyn Campbell
Katsuyo Thornton
Elizabeth Holm
Peter Gumbsch

TMS

Springer


TMS
ICME
MANUFACTURING
DESIGN
MATERIALS

Proceedings of the
2nd World Congress
on Integrated Computational Materials Engineering (ICME)

Sponsored by

TMS (The Minerals, Metals & Materials Society)

Held

July 7-11, 2013 at Salt Lake Marriott Downtown at City Creek, Salt Lake City, Utah

Edited by

Mei Li, Carelyn Campbell, Katsuyo Thornton, Elizabeth Holm, and Peter Gumbsch

Editors
Mei Li
Carelyn Campbell
Katsuyo Thornton
Elizabeth Holm
Peter Gumbsch

ISBN 978-3-319-48585-0 ISBN 978-3-319-48194-4 (eBook)
DOI 10.1007/978-3-319-48194-4

Chemistry and Materials Science: Professional

Published by Springer International Publishers, Switzerland, 2016
Reprint of the original edition published by John Wiley & Sons, Inc., 2013, 978-1-11876-689-7

Printed on acid-free paper

This Springer imprint is published by Springer Nature
The registered company is Springer International Publishing AG
The registered company address is: Gewerbestrasse 11, 6330 Cham, Switzerland

TABLE OF CONTENTS
2nd World Congress on Integrated Computational Materials Engineering

ICME Success Stories and Applications

Process Optimization

Materials Data for ICME

Building Blocks for ICME

ICME Challenges and Education

Preface

This is a collection of manuscripts presented at the 2nd World Congress on Integrated Computational Materials Engineering, a specialty conference organized by The Minerals, Metals & Materials Society (TMS) and the five conference organizers, and held in Salt Lake City, Utah, USA, on July 7-11, 2013.

Integrated Computational Materials Engineering (ICME) has received international attention as it has been proven to shorten product and process development time, while lowering cost and improving outcome. Building on the great success of the 1st Congress on Integrated Computational Materials Engineering in 2011 and the motivation of the Materials Genome Initiative (MGI) announced in June 2011, the 2nd World Congress on ICME convened researchers, educators, and engineers to assess the state-of-the-art ICME and determine paths to further the global advancement of ICME. Over 200 authors and attendees from all over the world contributed to this conference in the form of presentations, lively discussions, and papers presented in this volume. The international advisory committee members representing 14 different countries actively participated and promoted the conference.

The specific topics highlighted during this conference included ICME Success Stories and Applications with separate sessions on lightweighting, composites, ferrous, and non-ferrous applications; Process Optimization; Materials Data for ICME; Building Blocks for ICME with separate sessions on experimental tools, first principles and atomistic tools, computational thermodynamic and kinetics, process and performance modeling; and ICME Challenges and Education. The conference consisted of both all-conference single sessions and parallel sessions and integrated 10 keynote presentations from international experts, 2 panel discussions, 83 contributed presentations, and 70 poster presentations. From the two evening posters sessions, outstanding posters were selected for awards, which were presented to the authors at the conference dinner. The first panel discussion highlighted the need for the materials data infrastructure and initial efforts to develop such an infrastructure. The panel consisted of materials data experts from industry, academia, and government. The conference ended with a closing panel of experts focusing the discussion on the needed next steps forward to help ensure a broader and more global implementation of ICME in the future.

The 45 papers presented in these proceedings are divided into five sections: (1) ICME Success Stories and Applications; (2) Process Optimization; (3) Materials Data for ICME; (4) Building Blocks of ICME; and (5) ICME Challenges and Education. These manuscripts represent a cross section of the presentations and discussions from this conference. It is our hope that the 2nd World Congress on ICME and these proceedings will further the global implementation of ICME, broaden the variety of applications to which ICME is applied, and ultimately help industry design and produce new materials more efficiently and effectively.

Acknowledgements

The organizers/editors would like to acknowledge the contributions of a number of people without whom this 2nd World Congress, and the proceedings, would not have been possible.

First, we would like to offer many thanks to the TMS staff who worked tirelessly to make this an outstanding conference and excellent proceedings.

Second, we want to thank the international advisory committee for their input in the planning of the conference, the promotion of the conference, and their participation in the conference.

This international committee included:

John Ågren, KTH - Royal Institute of Technology, Sweden
John Allison, University of Michigan, USA
Dipankar Banerjee, Indian Institute of Technology, Bangalore, India
Yves Brechet, Institute National Polytechnic de Grenoble, France
Dennis Dimiduk, USAF Research Lab, USA
Masato Enomoto, Ibaraki University, Japan
Juergen Hirsch, Hydro Aluminum, Germany
Dorte Juul Jensen, Risoe National Laboratory, Denmark
Nack Kim, Pohang University of Science and Technology, Korea
Milo Kral, University of Canterbury, New Zealand
Peter Lee, Imperial College, United Kingdom
Baicheng Liu, Tsinghua University, China
Jiangfeng Nie, Monash University, Australia
Tresa Pollock, UC Santa Barbara, USA
Gary Purdy, McMaster University, Canada
Antonio J. Ramirez, Brazilian Synchrotron Light Laboratory, Brazil
K.K. Sankaran, Boeing Company, USA
James Warren, National Institute of Standards and Technology, USA
Deb Whitis, General Electric, USA

Finally, we would especially like to acknowledge the financial support of all our sponsors, especially ESI and UES, Inc. We are also grateful for the participation and contributions of all of the attendees.

Conference Editors/Organizers

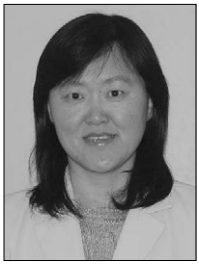

Mei Li is a Technical Expert and Group Leader of Light Metals Research and ICME at Ford Research and Advanced Engineering Laboratory. She is one of the key developers of Ford Virtual Aluminum Casting (VAC), a successful example of ICME applications in the automotive industry. The knowledge gained in metallurgy, physics, mechanics, and the computational models developed for microstructural evolution and property predictions in VAC have been extended to other materials and processes. This includes the development of computational tools for gear steels during the heat treatment process, high-pressure die casting of aluminum alloys for additional powertrain and body applications and high-pressure die casting of magnesium alloys for body applications. Her group is also developing advanced aluminum and heat-resistant alloys through ICME guidance and experimental validation as Ford continues to seek the competitive advantage in manufacturing lightweight, durable, and energy-efficient vehicles.

She received her Ph.D. degree from the Department of Materials and Metallurgy at McGill University in 2000. She has been actively involved in practicing, advancing, and promoting ICME and has organized numerous symposia, served as Technical Advisor for the ICME Committee within TMS, is a member of the Board of Review for the TMS journal *Integrating Materials and Manufacturing Innovation* (IMMI).

Carelyn Campbell is the acting group leader for the Thermodynamics and Kinetics group in the Materials Science and Engineering Division in the Material Measurement Laboratory at the National Institute of Standards and Technology (NIST). Her research is focused on diffusion in multicomponent multiphase systems and the development of data and informatics tools for phase-based data. For the past ten years, she has sponsored the NIST Diffusion Workshop series, which brings together experimentalists and theorists to improve the development of diffusion mobility databases and the prediction of diffusion controlled microstructure evolution in multicomponent multiphase systems. She received both her B.S. and Ph.D. in Materials Science and Engineering from Northwestern University. She began her tenure at NIST in 1997 as a National Research Council Postdoctoral Fellow. In 2010, she received a Bronze Medal from the Department of Commerce for superior federal service in leading the NIST Diffusion Workshop series.

Katsuyo Thornton is an associate professor of materials science and engineering at the University of Michigan, Ann Arbor. Her research focuses on computational studies of the evolution of microstructures and their effects in a wide range of materials, including metals, semiconductors, oxides, and biomaterials. She received her Ph.D. from the Department of Astronomy and Astrophysics at the University of Chicago in 1997. She was a Postdoctoral Fellow at Northwestern University and a Visiting Lecturer and Scientist at MIT, both in Materials Science and Engineering, followed by three years as a research assistant professor in Materials Science and Engineering at Northwestern University. She has organized numerous symposiums, and she was the primary guest editor of the *MRS Bulletin*, June 2008 issue on three-dimensional materials science. She also has served in a leadership role as the inaugural Chair of the Integrated Computational Materials Engineering (ICME) Committee within TMS. Transforming undergraduate and graduate education in materials science and engineering to include computational approaches is a passion of hers, which has led her to establish the Annual Summer School for Integrated Computational Materials Education with a grant from the National Science Foundation. To date, over 70 participants who are interested in incorporating computation into materials science and engineering curricula have attended the Summer School and associated short course. She is the recipient of several prestigious awards, including the TMS Early Career Faculty Fellow Award, NSF Faculty Early Career Development (CAREER) Award, and Carl Sagan Excellence in Teaching Award.

Elizabeth Holm is a professor of Materials Science and Engineering at Carnegie Mellon University. Prior to joining CMU in 2012, she spent 20 years as a computational materials scientist at Sandia National Laboratories, working on simulations to improve processes for lighting manufacture, microcircuit aging and reliability, and the processing and welding of advanced materials. Her research areas include the theory and modeling of microstructural evolution in complex polycrystals, the physical and mechanical response of microstructures, atomic-scale properties of internal interfaces, and the wetting and spreading of liquid metals. Dr. Holm obtained her B.S.E. in Materials Science and Engineering from the University of Michigan, S.M. in Ceramics from MIT, and dual Ph.D. in Materials Science and Engineering and Scientific Computing from the University of Michigan. Active in professional societies, Dr. Holm has received several honors and awards, is a Fellow of ASM International, is President of The Minerals, Metals & Materials Society for 2013–2014, is an organizer of several international conferences, and has been a member of the National Materials Advisory Board. Dr. Holm has authored or co-authored over 110 publications.

Peter Gumbsch received the diploma degree in physics in 1988 and his Ph.D. degree in 1991 from the University of Stuttgart. After extended visits at the Sandia National Laboratories in Livermore, postdoctoral work at the Imperial College, London and the University of Oxford he returned to the Max-Planck-Institute in Stuttgart as a group leader and established the group Modeling and Simulation of Thin Film Phenomena. In 2001 he took the chair for Mechanics of Materials at Karlsruhe Institute of Technology KIT and the position as head of Fraunhofer Institute for Mechanics of Materials IWM in Freiburg and Halle.

His research activities focus on modeling and simulation of materials, in particular multiscale modeling approaches. The intention is to make materials and components safer, more reliable, and more durable. He and his team are pioneering the integration of material modeling in the product development process. His current interest is in the investigation of friction and wear processes, where complex interactions of mechanics, physics, and chemistry are important. The aim is to improve material and energy efficiency in technical systems.

Among other recognitions he was awarded the Masing Memorial Award (1998) and the Gottfried Wilhelm Leibniz Prize (2007). He is chairman of the section Engineering Sciences of the German Academy of Sciences Leopoldina. In 2009 he was nominated as Hector Fellow and in 2011 he was appointed as Advisory Professor of Shanghai Jiao Tong University, China.

2nd World Congress

on Integrated Computational Materials Engineering (ICME)

ICME Success Stories and Applications

2nd World Congress on Integrated Computational Materials Engineering
Edited by: Mei Li, Carelyn Campbell, Katsuyo Thornton, Elizabeth Holm, and Peter Gumbsch
TMS (The Minerals, Metals & Materials Society), 2013

APPLICATION OF COMPUTATIONAL THERMODYNAMICS AND CALPHAD IN MAGNESIUM ALLOY DEVELOPMENT

Alan A. Luo

General Motors Global Research and Development
30500 Mound Road, Warren, MI 48090, U.S.A.

Keywords: Magnesium alloy, CALPHAD, computational thermodynamics, alloy development

Abstract

This paper presents two examples of using computational thermodynamics and CALPHAD modeling in the selection and development of new magnesium alloys. The Scheil model simulation of the solidification microstructure suggests that calcium is more effective than rare earth elements (such as cerium) in suppressing the formation of $Mg_{17}Al_{12}$ phase in binary Mg-Al alloys. Calcium additions also introduce more thermally stable phases in the ternary alloys, thus improving their creep resistance and strength at elevated temperatures.

Introduction

Application of lightweight materials is a cornerstone for all major automakers to address the challenging fuel economy targets recently set for the industry. Magnesium, the lightest structural metal, will thus see increased use in a wide range of structural and functional applications for energy generation, energy storage, propulsion, and transportation [1]. Current applications of magnesium alloys are limited to non-structural or semi-structural components in the transportation industry, due to limited mechanical properties of conventional Mg-Al-based alloys such as AZ91 (Mg-9Al-1Zn[1]) and AM60 (Mg-6Al-0.3Mn). New magnesium alloys are being developed with higher strength, ductility and creep resistance at room and elevated temperatures [2-9].

While most alloy development has occurred through meticulous experiments and microstructure-composition relationships, recent approaches rely on computational methods based on phase diagrams for materials design and process optimization. These methods allow for efficient manipulation of alloy composition and process parameters to achieve the desired microstructure and properties. Originated from the early work of Kaufman and Bernstein [10], the CALPHAD (CALculation of PHAse Diagrams) technique, based on computational thermodynamics of alloy systems, has matured over the past few decades; and many commercial software packages, such as ThermoCalc [11], FactSage [12] and Pandat [13], have become important ICME (integrated computational materials engineering) tools used in the development of new materials and products [14]. This paper demonstrates two examples of applying computational thermodynamics and CALPHAD modeling in the development of new creep-resistant magnesium alloys using Pandat8.1 code and its PanMg2012 database.

Computational Thermodynamics

The CALPHAD approach is based on the thermodynamic description of an alloy system, which denotes a set of thermodynamic parameters for all phases in the system. In a ternary alloy

[1] All compositions in wt.% except otherwise stated.

system, the phases of interest are solid, liquid and intermetallic phases. The Gibbs energy per mole of a liquid or a substitutional solid solution is [16],

$$G_m^{\phi} = \sum_i x_i {}^{\circ}G_i^{\phi} + RT\sum_i x_i \ln x_i + \Delta^{xs}G_m^{\phi} \quad (1)$$

The first term on the right-hand side (RHS) of Eq. (1) is the Gibbs energy of the component elements in the reference state at a constant temperature (T) and a pressure (P) of 1 bar, the second is the ideal Gibbs energy of mixing, and the third the excess Gibbs energy. The last term is described by the Redlich-Kister equation as given below. The number of parameters is limited to three at a constant T and P of 1 bar.

$$\Delta^{xs}G_m^{\phi}(x_i, T) = x_i x_j \sum_{\nu=0}^{\nu=2} {}^{(\nu)}\lambda (x_i - xj_j)^{\nu} \quad (2)$$

The symbols G_m, R, λ, x_i, x_j are, respectively, the molar Gibbs energy, universal gas constant, model parameters, mole fraction of component i and that of component j. For the intermetallic phases with more than one sublattice, the compound energy formalism is used and given below:

$$G_m = \sum y_p^{(i)} y_q^{(j)} G_{(pq)} + RT\sum f_i y_p^{(i)} \ln y_p^{(i)} + \sum y_p^{(i)} y_q^{(i)} y_r^{(j)} \sum_k L_{(p,qr)}^{(k)} (y_p^{(i)} - y_q^{(i)})^k \quad (3)$$

where G_m is the Gibbs energy expressed as a function of the concentrations of the sublattice species. The first term on the RHS of Eq. (3) is the reference term, the second ideal Gibbs energy of mixing on the sublattices, and the last term the excess Gibbs energy on the sublattice. The y's are the mole fractions of the species on a specific sublattice, f_i the fraction of a specific sublattice within the crystal, and $L_{(p,q:r)}$'s are the model parameters. The superscripts (i), (j) specify the sublattice in question and the subscripts p and q the species on the sublattices.

The above descriptions of alloy systems were coded in the Pandat [14] software for phase equilibria calculations in this paper. The latest thermodynamic database PanMg8 was used in the calculations.

Magnesium Alloy Development

Mg-Al System

Aluminum is the most widely used alloying addition in magnesium for strengthening and castability. Fig. 1 shows the calculated Mg-Al phase diagram. There are two eutectic reactions that are important to the phase constitution of Mg-Al binary alloys:

1) At 450°C L → Al + Mg_2Al_3
2) At 436°C L → Mg + $Mg_{17}Al_{12}$

Commercial cast and wrought magnesium alloys (AZ91, AM60 and AZ31) contain less than 10% Al, and the microstructure of these Mg-Al based alloys is generally characterized by the formation of $Mg_{17}Al_{12}$ phase. The low eutectic temperature (436°C) of $Mg_{17}Al_{12}$ phase limits the application of Mg-Al alloys to temperatures below 125°C, above which the discontinuous precipitation the $Mg_{17}Al_{12}$ phase leads to substantial creep deformation [2]. Therefore, possible approaches for improving creep resistance in Mg-Al based alloys include: 1) suppressing the formation of the $Mg_{17}Al_{12}$ phase; 2) pinning grain boundary sliding; and 3) slowing solute diffusion in the magnesium matrix.

Mg-Al-Ce System

Earlier experimental work [7, 17] has shown that additions of RE in the form of mischmetal can improve the creep resistance of Mg–Al based alloys, especially when the aluminium content was low (less than 4%). This led to the development of AE series alloys, AE42 (Mg-4Al-2RE) and AE44 (Mg-4Al-2RE) where the mischmetal RE generally contains more than 60%Ce (balance La, Nd and Pr). Fig. 2 shows the calculated liquidus projection of the Mg-Al-Ce system in the Mg-rich corner. Generally, the liquidus temperature decreases with Al addition (up to at least about 10%) and Ce (up to at least about 10%), with the following two type II invariant reactions marked at 871K (598°C) and 835K (562°C), respectively:

1) At 598°C $L + (Al,Mg)_{12}Ce \rightarrow Mg + Mg_{12}Ce$
2) At 562°C $L + (Al,Mg)_{12}Ce \rightarrow Mg + Al_{11}Ce_3$

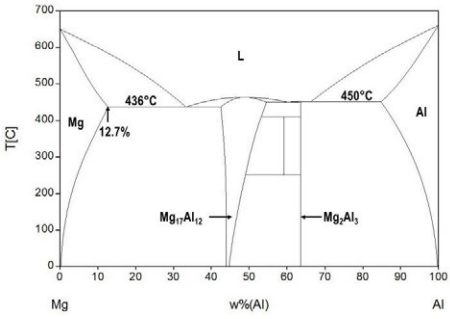

Fig. 1. Calculated Mg-Al phase diagram.

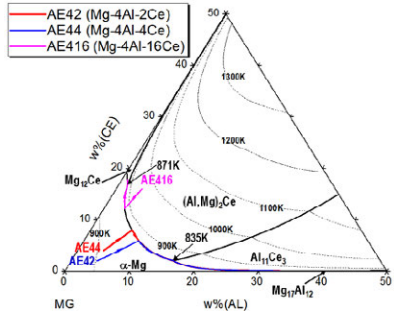

Fig. 2. Calculated Mg-Al-Ce liquidus projection and solidification paths of experimental Mg-Al-Ce alloys.

The calculated solidification paths of AE42 and AE44 alloys using the Scheil model, based on the assumption of complete mixing in the liquid but no diffusion in the solid, are superimposed in the phase diagram shown in Fig. 2. Based on the simulation results, the solidification sequence for both alloys is as follows:

1) Nucleation of primary magnesium: $L \rightarrow L + Mg$
2) Binary eutectic reaction: $L \rightarrow L + Mg + (Al,Mg)_{12}Ce$
3) Type II invariant reaction: $L + (Al,Mg)_{12}Ce \rightarrow L + Mg + Al_{11}Ce_3$
4) Ternary eutectic reaction: $L \rightarrow Mg + Al_{11}Ce_3 + Mg_{17}Al_{12}$

It is clear that the additions of 2-4% Ce to Mg-Al alloys have resulted in the formation of $Al_{11}Ce_3$ in addition to the $Mg_{17}Al_{12}$ phase in the Mg-Al binary system. Fig. 3(a) shows the effect of Ce addition to Mg-4Al alloy on the fraction of $Mg_{17}Al_{12}$ phase in the ternary alloy as calculated using the Scheil model. This indicates that it takes about 15% Ce to completely suppress the formation of $Mg_{17}Al_{12}$ phase in the Mg-4Al alloy. Similar calculations were made for Mg-Al-Ce alloys with various Al and Ce contents, Fig. 3(b), which can be used as guidance to design the ternary alloy avoiding $Mg_{17}Al_{12}$ phase formation for elevated temperature

applications. Fig. 2 also shows the solidification sequence of AE416 (Mg-4Al-16Ce) alloy as follows:

1) Nucleation of $(Al,Mg)_{12}Ce$ phase: $L \rightarrow L + (Al,Mg)_{12}Ce$
2) Binary eutectic reaction: $L \rightarrow L + Mg + (Al,Mg)_{12}Ce$
3) Type II invariant reaction: $L + (Al,Mg)_{12}Ce \rightarrow L + Mg + Mg_{12}Ce$
4) Binary eutectic reaction: $L \rightarrow Mg + Mg_{12}Ce$

The eutectic temperatures for $Al_{11}Ce_3$, $(Al,Mg)_{12}Ce$ and $Mg_{12}Ce$ phases are calculated as 560°C, 622°C and 867°C, respectively; which are all significantly higher than of the $Mg_{17}Al_{12}$ phase (436°C). The Scheil model was also used to calculate the fraction of phases formed in the three AE alloys according to the above solidification paths. The results of these calculations are summarized in Table 1 and compared with commercial AM50 (Mg-5Al-0.3Mn) alloy. In AE alloys, 4-5%Al is generally needed for die castability, while it is very expensive to use 16%Ce (e.g., AE416 alloy) to suppress formation of $Mg_{17}Al_{12}$. On the other hand, AE44 alloy has significantly lower fraction of $Mg_{17}Al_{12}$, and, thus, much better high-temperature strength compared with AE42 or AM50 alloy [18]. Therefore, AE44 alloy was selected for the Corvette engine cradle application where the operating temperature would approach 150°C [19].

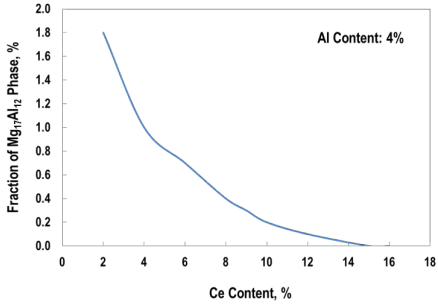

Fig. 3(a). Effect of Ce content on the fraction of $Mg_{17}Al_{12}$ phase in Mg-4Al-Ce alloys following solidification based on the Scheil simulation.

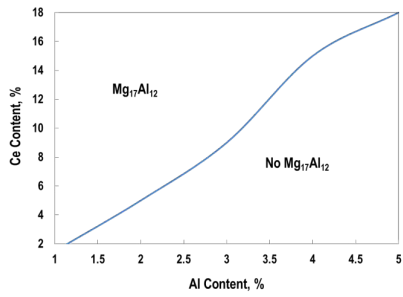

Fig. 3(b). Effect of Ce and Al content on the formation of $Mg_{17}Al_{12}$ phase in Mg-Al-Ce alloys following solidification based on the Scheil simulation.

Mg-Al-Ca System

Mg-Al-Ca system was investigated to replace the more expensive AE alloys. Fig. 4 shows the calculated liquidus projection of the Mg-Al-Ca system, superimposed by the solidification paths of three Mg-Al-Ca alloys; AX51 (Mg-5Al-1Ca), AX52 (Mg-5Al-2Ca) and AX53 (Mg-5Al-3Ca), calculated using the Scheil model. Based on the simulation results, the solidification sequence for AX51 and AX52 alloys are as follows:

Table 1. Scheil simulation (vol.%) of Mg-Al-Ce alloys (Baseline: AM50 alloy)

Alloy	$(Al,Mg)_2Ce$	$Al_{11}Ce_3$	$Mg_{17}Al_{12}$	$Mg_{12}Ce$
AM50	-	-	4.3	
AE42	0.9	0.2	1.8	
AE44	2.0	0.1	1.0	
AE416	9.5	0	0	0.7

1) Nucleation of primary magnesium: $L \rightarrow L + Mg$

2) Binary eutectic reaction: $L \rightarrow L + Mg + (Mg,Al)_2Ca$
3) Type II invariant reaction: $L + (Mg,Al)_2Ca \rightarrow L + Mg + Mg_{17}Al_{12}$
4) Binary eutectic reaction: $L \rightarrow Mg + Mg_{17}Al_{12}$

AX53 alloy has a different ternary eutectic reaction where Mg_2Ca is formed instead of $Mg_{17}Al_{12}$, resulting in a slightly different solidification path:

1) Nucleation of primary magnesium: $L \rightarrow L + Mg$
2) Binary eutectic reaction: $L \rightarrow L + Mg + (Mg,Al)_2Ca$
3) Ternary eutectic reaction : $L \rightarrow Mg + (Mg,Al)_2Ca + Mg_2Ca$

Fig. 5(a) shows the effect of Ca on the fraction of $Mg_{17}Al_{12}$ phase formed in these alloys during solidification as determined by the Scheil simulation. It is evident that the Ca content has to be greater than 2.8% in order to completely suppress the formation of $Mg_{17}Al_{12}$ in the Mg-5Al alloy. Furthermore, the critical Ca contents were calculated for Mg-Al-Ca ternary alloys containing 3-9% Al, and plotted in Fig. 5(b), which is an important composition map for optimizing creep-resistant alloys in this system.

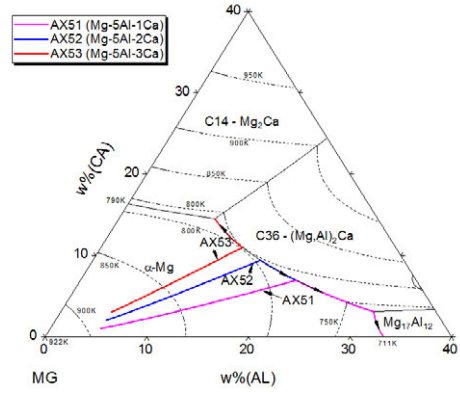

Fig. 4. Calculated Mg-Al-Ca liquidus projection and the solidification paths of the experimental Mg-Al-Ca alloys.

The presence of $(Mg,Al)_2Ca$ phase in the die-casting microstructure of Mg-Al-Ca alloys [20] and Mg_2Ca eutectic phase in AX53 (die casting) have been confirmed in previous experimental results [20, 21]. While C14 is a complete hcp (hexagonal close packed) structure with 100% hexagonality, C36 is an intermediate structure between hcp and fcc (face centered cubic) with 50% hexagonality [2]. The role of C14 and C36 phases in creep resistance of Mg-Al-Ca-based alloys has been discussed in previous investigations [20, 21]. The calculated Mg-Ca binary diagram suggests that the C14 phase has a high eutectic temperature (517°C) and melting point (710°C) and can thus exhibit better thermal stability. The C36 phase is more stable than C14 and $Mg_{17}Al_{12}$ phases in terms of the relative change in the eutectic structure during annealing. This implies an advantage of the C36 phase as a strengthener at grain boundaries in creep-resistant alloys. This computational alloy design approach confirms the 2-3% Ca present in these alloys to have significant fractions of C14 and C36 phases for creep resistance, and the AX53 alloy to have improved castability due to its reduced freeze range compared with AX51 and AX52 alloys [22]. AX53 alloy is presently being developed by GM for automotive powertrain applications.

Summary

Computational thermodynamics and CALPHAD modeling, when combined with critical experimental validation, can be used to guide the selection and development of new magnesium alloys. Ca is more effective than RE elements (such as Ce) in suppressing the formation of $Mg_{17}Al_{12}$ phase in binary Mg-Al alloys and introducing more thermally stable phases in the ternary alloys; thus, improving their creep resistance and strength at elevated temperatures. AE44 alloy is used in engine cradle applications and AX53 alloy is being developed by GM for automotive powertrain applications.

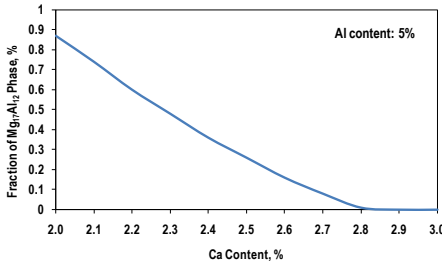

Fig. 5(a). Effect of Ca content on the fraction of $Mg_{17}Al_{12}$ phase in Mg-4Al-Ca alloys following solidification based on the Scheil simulation.

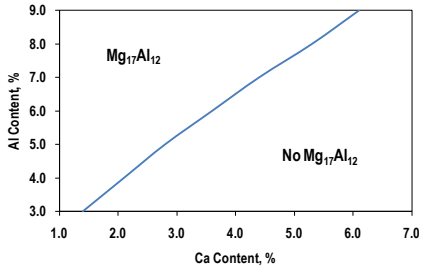

Fig. 5(b). Effect of Ca and Al content on the formation of $Mg_{17}Al_{12}$ phase in Mg-Al-Ca alloys following solidification based on the Scheil simulation.

References

1. T.M. Pollock, Science, 2010, 328, 986.
2. A.A. Luo, International Materials Reviews, 2004, 49, (1), 13.
3. P. Bakke, K. Pettersen, D. Albright, in Magnesium Technology 2004, TMS, 289.
4. S. Cohen, et al G.R. Goren-Muginstein, S. Avraham, G. Dehm, M. Bamberger, in Magnesium Technology 2004, TMS, 301.
5. A.L. Bowles, C. Blawert, N. Hort, K.U. Kainer, in Magnesium Technology 2004, TMS, 307.
6. A.A. Luo and A.K. Sachdev, in Magnesium Technology 2009, TMS, 437.
7. P. Bakke and H. Westengen, in Magnesium Technology 2005, TMS, 291.
8. P. Lyon, T. Wilks, I. Syed, in Magnesium Technology 2005, TMS, 203.
9. M.S. Dargusch, K. Pettersen, K. Nogita, M.D. Nave, G.L. Dunlop, Met. Trans., 47, 2006, 977.
10. L. Kaufman, H. Bernstein, Computer calculation of phase diagrams, New York, Academic Press, 1970.
11. http://www.thermocalc.com/
12. http://www.factsage.com/
13. http://www.computherm.com/
14. Y.A. Chang, S. Chen, F. Zhang, X. Yan, F. Xie, R. Schmid-Fetzer, W.A. Oates, Prog. Mater. Sci., 2004, 49, 313.
15. A.A. Luo, R.K. Mishra, B.R. Powell, A.K. Sachdev, Materials Science Forum, 2012, 706-709, 69.
16. Pandat 8.0 - Phase Diagram Calculation Software for Multi-component Systems, CompuTherm LLC, Madison, WI, USA, 2008.
17. W.E. Mercer II, SAE Technical Paper 900788, Society of Automotive Engineers, Warrendale, PA, USA, 1990.
18. A.A. Luo, keynote talk, Magnesium Technology 2012 Symposium, TMS Annual Meeting, Orlando, FL, USA, March 11-15, 2012.
19. J. Aragones, K. Goundan, S. Kolp, R. Osborne, L. Ouimet, W. Pinch, SAE Technical Paper No. 2005-01-0340, SAE International, Warrendale, PA, USA, 2005.
20. A.A. Luo, M.P. Balogh, B.R. Powell, Metall Mater Trans A, 2002, 33, 567.
21. A. Suzuki, N.D. Saddock, J.W. Jones, T.M. Pollock: Acta Materialia, 2005, 53, 2823.
22. A.A. Luo, B.R. Powell, A.K. Sachdev, Intermetallics, 2012, 24, 22.

2nd World Congress on Integrated Computational Materials Engineering
Edited by: Mei Li, Carelyn Campbell, Katsuyo Thornton, Elizabeth Holm, and Peter Gumbsch
TMS (The Minerals, Metals & Materials Society), 2013

MODELLING PRECIPITATION KINETICS DURING AGING OF AL-MG-SI ALLOYS

Qiang Du[1], Jepser Friis[1]

[1]SINTEF Materials and Chemistry, Trondheim, Norway

Keywords: precipitation kinetics modeling, Al-Mg-Si alloys, KWN model, morphology change

Abstract

A classical Kaufmann-Wagner numerical model is employed to predict the evolution of precipitate size distribution during the aging treatment of Al-Mg-Si alloys. One feature of the model is its fully coupling with CALPHAD database, and with the input of interfacial energy from ab-initial calculation, it is able to capture the morphological change of the precipitates. The simulation results will be compared with the experimental measurements.

Introduction

The Al-Mg-Si (6xxx) aluminium alloys, with 1-2wt% Mg and Si added to pure Al, have been widely used in construction, automobile, and marine industries due to their excellent properties (high strength/weight ratio, good formability and weldability, and excellent corrosion resistance). They are age harden-able, and the increase in strength results from the precipitation of different types of metastable phases. Experimental investigations [1] have shown that the hardening process in very complex and difficult to optimize as many parameters including alloy composition, heating rate, aging temperature and time, solution treatment temperature and cooling rate from solution, storing time at room temperature prior to aging are involved. To optimize the hardening process, great efforts have been made to develop a predictive integrative through process model [2], which consists of solidification microstructure microsegregation model, meso-scale precipitate kinetics model, solute and precipitation hardening model, etc.

The focus of this paper is to improve one important chain of the integrative model, i.e., the meso-scale precipitation model. The one that have been used is based on the numerical framework developed by Kampmann and Wagner [3] (referred to as KWN model). The essence of this model as well as its later variants is that the continuous Particle Size Distribution (PSD) curve is subdivided into size classes, each of which is associated with a precipitate number. The temporal evolution of size distribution is then tracked by following the size evolution of each discrete size class. The KWN framework has been used in various alloys systems with modifications related to the treatment of the Gibbs Thompson effect and the numerical solution procedures [4,5, 6,7,8,9, 10]. However, one assumption adopted in the model, i.e., precipitates being of spherical shape, has restricted its usage to the alloy systems such as AA6xxx alloys where precipitates are of needle shape. The aim of this paper is to remove this restriction and apply the extended model to simulate precipitation of needle-shape precipitates.

In the ealier work due to Frank S. Ham [11], the needle-shape precipitate were approximated as prolate spheroid, and a simple equation was derived which describes the diffusional flux that brings in solute to a growing precipitate by employing a variational method. Ham's work has been confirmed very recently with the computational experiments by phase field method for systems with small anisotropy and small super-saturations in [12]. However Ham did not

consider Gibbs-Thomson effect and his model was only for binary alloys. Phase field model is also capable of modeling the growth and morphological evolution of several non-spherical precipitates, but it is still beyond the computational power of a personal computer for phase filed model to handle concurrent nucleation, growth and coarsening of multi-component alloys. In this paper, we will firstly extend Ham's treatment to take into account Gibbs-Thomson effect of multi-component alloys. Then the extended model is combined with empirical morphological evolution law to simulate precipitation kinetics of needle-shape precipitates during aging treatment of AA6xxx alloys.

Model Description

Experimentally it has been observed that precipitates during aging treatment of AA6xxx alloys are of needle-shape. Follow Ham's treatment, a needle-shape precipitate is approximated by a prolate spheroid with length of L and radius of r_0:

$$\frac{x^2}{b^2}+\frac{y^2}{b^2}+\frac{z^2}{a^2}=1 \tag{1}$$

Where $a=\frac{L}{2}, b=r_0$. The aspect ratio, α, eccentricity e, volume, V, and surface area, S, of the prolate precipitate are given by:

$$\alpha=\frac{L/2}{r_0} \tag{2.a}$$

$$e=\sqrt{1-\frac{4{r_0}^2}{L^2}} \tag{2.b}$$

$$V=\frac{4\pi a^3}{3}(1-e^2) \tag{2.c}$$

$$S=2\pi {r_0}^2(1+\frac{a}{r_0 e}sin^{-1}e) \tag{2.d}$$

In general α is much larger than 1, and e is close to unity.

It is useful to find the radius, R, of an equivalent sphere, whose volume is identical to the prolate:

$$R=a\sqrt[3]{1-e^2} \tag{3}$$

As to be shown later, the precipitation kinetics of the prolate and its equivalent sphere are closely related.

As in the case of the growth of spherical precipitate, it is assumed that the compositional profile of solute i in the front of the migrating precipitate-matrix interface satisfies the steady state diffusion equation:

$$\nabla^2 c_i(x)=0 \tag{4}$$

By introducing of spheroidal coordinate, the compositional profile surrounding a growing prolate could be described [11]:

$$c_i(x)=c_i^m+\Delta c_i(1-\frac{\ln\frac{(x+1)(x_0-1)}{(x-1)(x_0+1)}}{\ln\frac{(x_S+1)(x_0-1)}{(x_S-1)(x_0+1)}}) \tag{5}$$

Where $c_i(x)=c_i^m+\Delta c_i$ on the prolate surface $x=x_0$, and $c_i(x)=c_i^m$ for large $x\sim x_s$

Eq. (5) should be contrasted with the compositional profile surrounding the equivalent spherical precipitate:

$$c_i^{Spherical}(x) = c_i^m + \Delta c_i \frac{L}{2} \frac{\sqrt[3]{1-e^2}}{x} \tag{6}$$

With the variational method, Ham [11] derived the following equation describing the flux that brings in solute to the growing particle:

$$J_i^m = \frac{4\pi D_i \Delta c_i L e}{\ln \frac{1+e}{1-e}} \tag{7}$$

Eq. (7) should be contrasted with its counter-part for the equivalent spherical precipitate:

$$J_i^{mSpherical} = 4\pi D_i \Delta c_i \frac{L}{2} \sqrt[3]{1-e^2} \tag{8}$$

With the solute conservation law, the rate of the volume change of the prolate could be derived from Eq.(7):

$$J_i^m dt = (c_i^m + \Delta c_i - c_i^p) dV \tag{9.a}$$

$$\dot{V} = \frac{4\pi D_i \Delta c_i L e}{\ln \frac{1+e}{1-e} (c_i^m + \Delta c_i - c_i^p)} \tag{9.b}$$

Eq.(9) allows for the tracking of the evolution of precipitate volume providing Δc_i is known. It is trivial to calculate Δc_i for binary alloys in the absence of Gibbs-Thomson effect. However, as pointed out by Mou and Howe in [13], Gibbs-Thomson effect would modify Δc_i along the precipitate interface due to the local curvature:

$$\gamma = \frac{\frac{L}{2}\left(2{r_0}^2 + \left(\frac{L^2}{4} - {r_0}^2\right) cos^2\beta\right)}{2r_0 \left({r_0}^2 + \left(\frac{L^2}{4} - {r_0}^2\right) cos^2\beta\right)^{3/2}}, -\frac{\pi}{2} < \beta < \frac{\pi}{2} \tag{10}$$

Obviously the local curvature depends on β, so-called parametric latitude. To simplify the mathematical treatment, the local variation is treated in an average way, i.e., we assume that the modification to the interfacial matrix composition on the whole prolate surface is represented by the mean curvature of the prolate surface. This assumption may be justified by short-circuit effect originated from fast diffusion along the migrating surface. More rigorous treatment with the variational method is under development. Therefore we have

$$\gamma_{mean} = \frac{1}{\pi} \int_{-\frac{\pi}{2}}^{\frac{\pi}{2}} \frac{\frac{L}{2}\left(2{r_0}^2 + \left(\frac{L^2}{4} - {r_0}^2\right) cos^2\beta\right)}{2r_0 \left({r_0}^2 + \left(\frac{L^2}{4} - {r_0}^2\right) cos^2\beta\right)^{\frac{3}{2}}} d\beta \tag{11}$$

Fig. 1 plots the dependence of the normalized mean curvature, $\hat{\gamma}_{mean}$, on aspect ratio where $\hat{\gamma}_{mean} = \frac{\gamma_{mean}}{\frac{1}{R}}$. Clearly the curvature effect is more significant than in the equivalent spherical

precipitate. With this assumption it is possible to obtain Δc_i together with kinetic constrains and local equilibrium assumption.

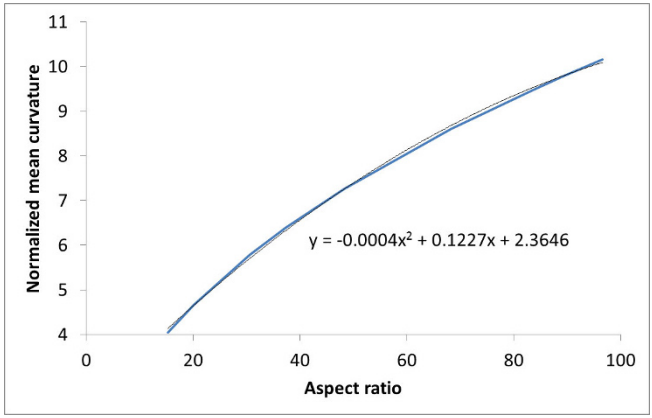

Fig. 1 the dependence of the normalized mean curvature on aspect ratio

Theoretically the evolution of aspect ratio could be due to anisotropy in interfacial energy such as in the case of the development of dendrite during solidification. Other factors might be contributing too. For example one could speculate that preferential growth occurs at the needle tip while thickening of the cross section is slow. It might be possible for the entire surface of the particle serves to capture solute atom from solution, and there might be a mechanism to transport them to the active region of the surface [14]. It is a very interesting topic to be investigated with phase field model while our treatment of the evolution of aspect ratio is of empirical nature. Experimentally it is known [15] that aspect ratio is not constant but scale with the size parameter of the cross section of the precipitate, *d*, i.e.,

$$\alpha = 14\, nm^{-1}\, d \tag{12}$$

Finally some words on the phase diagram used in our simulation. The coupling with CALPHAD method has been implemented to get access to multi-component phase diagram. Our final goal is to simulate the precipitation of β" phase. However the simulations to be reported in the next section are performed for Mg_2Si phase due to the unavailability of the relevant metastable phase diagram. The construction of the metastable phase diagram for β" is in progress.

Results and Discussions

The input parameters use in the simulations are listed in Table 1.

Table 1. The input parameters used in the simulations

Surface energy (J/m^2)	Molar volume (m^3)	Thermodynamic database	aging temperature	Mg and Si Diffusivity within matrix phase (m^2/s) [16]	
0.24	1.0×10^{-5}	TTAL6*	250 °C	1.9×10^{-19}	3.8×10^{-19}

* TTAL6 is the Al-based alloys database developed by Thermotech, Surrey, UK.

The first simulation is for the growth of single small prolate precipitate from the center of a finite volume of 0.0072 μm^3 (corresponding a sphere with a diameter of 240 nm). Initially the precipitate has a r_0 of 0.5 nm and aspect ratio of 7.2. It grows for about 30 minutes to r_0 of 6.2 nm and aspect ratio of 86. The predicted precipitate fraction evolution curve is plotted in Fig. 2 together with the one for a spherical precipitate (i.e., with constant aspect ratio equal to 1) growing in the identical conditions. Both of the two curves approaches to the final equilibrium fraction (1.06%), but the prolate precipitate grows much faster than the spherical one.

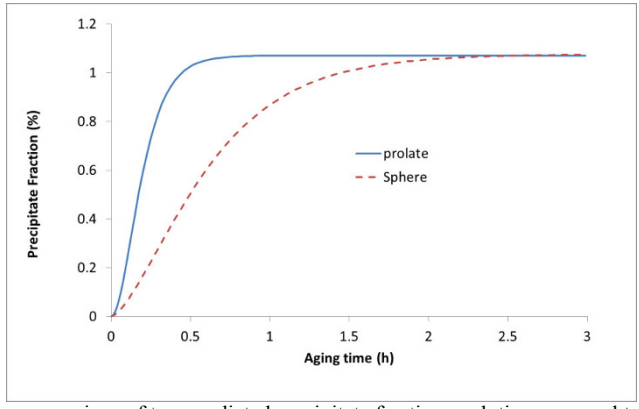

Fig. 2 The comparison of two predicted precipitate fraction evolution curves obtained with different approximations of precipitate shape (prolate and sphere) for the growth of single Mg2Si precipitate at 250 °C from Al-0.65wt%Mg-0.59wt%Si solid solution.

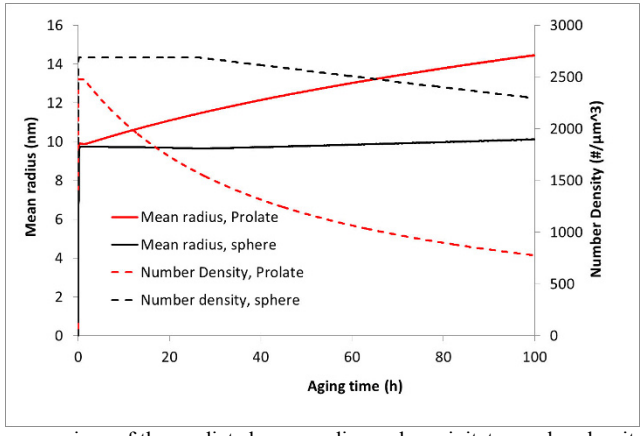

Fig. 3 The comparison of the predicted mean radius and precipitate number density evolution curves obtained with different approximations of precipitate shape (prolate and sphere) for the aging treatment of Al-0.65wt%Mg-0.59wt%Si at 250 °C.

The second group of simulations is for the aging treatment of Al-0.65wt%Mg-0.59wt%Si at 250 °C. Concurrent precipitate nucleation, growth, and coarsening have been taken into account. The predicted mean radius and number density are plotted in Fig. 3. Clearly after 100 hours aging treatment significant coarsening occurs in the simulation with prolate shape precipitate while negligible coarsening in the one with spherical precipitates. It implies better agreement could be obtained with the experimental results reported in [1] where significant coarsening was observed after only 3 hours of aging heat treatment.

Conclusions

The KWN model has been extended to take into account the effect of precipitate shape on precipitation kinetics during aging treatment of Al-Mg-Si alloys. In the proposed model the growth rate of a prolate shape precipitate, in comparison to a spherical precipitate with identical volume, is magnified by a factor of $\frac{\frac{2}{\sqrt[3]{1-e^2}}e}{\ln\frac{1+e}{1-e}}$, where e is eccentricity. Its curvature effect is magnified by a factor of $-00044\alpha^2 + 0.122\alpha + 2.36$, where α is aspect ratio.

The model has been applied to simulate the aging experiments reported in the literature, and reasonable agreements have been obtained. Further improvement is required to handle shape coarsening.

Acknowledgement

The financial support from the Research Council of Norway under the eVITA programme with contract number of NFR Project 205353/V30 "Multiscale Modelling of hardening Precipitate Interfaces in Alloy Design" is gratefully acknowledged.

[1] C. D. Marioara, H. Nordmark, S. J. Andersen, R. Holmestad, "Post-β" phases and their influence on microstructure and hardness in 6xxx Al-Mg-Si alloys", J. Mater. Sci 41 (2006) 471-478.
[2] Myhr, Ole Runar; Grong, Oystein; Pedersen, Ketill Olav, "A Combined Precipitation, Yield Strength, and Work Hardening Model for Al-Mg-Si Alloys", METALLURGICAL AND MATERIALS TRANSACTIONS A-PHYSICAL METALLURGY AND MATERIALS SCIENCE Volume: 41A Issue: 9 Pages: 2276-2289.
[3] Wagner R, Kampmann R. Homogeneous second phase precipitation, in: Cahn RW (Eds.). Materials Science and technology: a comprehensive treatment, Weinheim: John Wiley & Sons Inc.; 1991.
[4] Maugis P, Goune M. Acta Materialia 2005; 53: 3359.
[5] Myhr OR, Grong O. Acta Materialia 2000; 48: 1605.
[6] Robson JD. Acta Materialia 2004; 52: 4669.
[7] Gandin CA, Jacot A. Acta Materialia 2007; 55: 2539.
[8] Perez M, Dumont M, Acevedo-Reyes D. Acta Materialia 2008; 56: 2119.
[9] Kamp N, Sullivan A, Tomasi R, Robson JD. Acta Materialia 2006; 54: 2003.
[10] Q. Du, W. Poole, M. Wells, "A mathematical model coupled to CALPHAD to predict precipitation kinetics for multicomponent aluminum alloys", Acta Materialia 60 (2012) 3830-3839.
[11] Frank S. Ham, "Theory of diffusion-limited precipitation", J. Phys. Chem. Solids, 1958, Vol.6. pp335-351.
[12] Rajdip Mukherjee, T.A. Abinandanan, M. P. Gururajan, "Phase field models as computer experiments: Growth kinetics of anisotropic precipitates", Materials Science Forum, Volume: Advances in Materials Development, 2013.
[13] Y. Mou, J. M. Howe, "Diffusion fields associated with prolate spheroids in size and shape coarsening", Acta Mater. Vol. 45, No. 2, pp.823-835.
[14] Frank S. Ham, "Diffusion-limited growth of precipitate particles", Journal of applied physics, Volume 30, number 10, October 1959. 1518-1525.
[15] J. Friis, internal report, 2012.
[16] Y. Du et al, "Diffusion coefficients of some solutes in fcc and liquid Al: critical evaluation and correlation", Materials Science and Engineering A363 (2003) 140-151.

2nd World Congress on Integrated Computational Materials Engineering
Edited by: Mei Li, Carelyn Campbell, Katsuyo Thornton, Elizabeth Holm, and Peter Gumbsch
TMS (The Minerals, Metals & Materials Society), 2013

MODELING PROCESSING-PROPERTY RELATIONSHIPS TO PREDICT FINAL ALUMINUM COIL QUALITY

Kai F. Karhausen, Galyna Laptyeva, Stefan Neumann

Hydro Aluminium Rolled Products GmbH
R&D, Georg-von-Boeselager-Str. 21
53117 Bonn, Germany

Keywords: Aluminum, Rolling, Process Simulation, Property Simulation

Abstract

In the definition of the term ICME the integration of multiple length-scale models is the key requisite to obtain information required to design products. While product properties are a measure on a macroscopic length scale, they are controlled by the microstructure on a microscopic or even atomistic length-scale. They are generated on production facilities on a very large scale.

In translation of the definition of ICME to the production of rolled Aluminum semi-fabricated products alloys and processing routes must be combined to deliver improved final customer properties to enable the development of new designs and products. Since the relationships between processing conditions, microstructural evolution and derived properties are highly non-linear, this task can only be achieved by computer aided methods.

Critical properties of Aluminum coils and sheet are on the one hand the physical and chemical properties of the metal, such as strength, elongation, anisotropy, formability, corrosion resistance etc.. But on the other hand, geometrical tolerances and surface quality are equally important and often result from metallurgical events during processing. In some cases they can be derived from integrated process and microstructure simulation methods as well.

This paper describes the state of the art in through process modeling of Aluminum coils and strip with a view of tracing the microstructural development and deriving property information. Especially new approaches to critical parameters such as coil stability and sheet flatness, resulting from microstructural mechanisms are treated by sample computations of industrial processing chains.

Introduction

The properties of aluminum wrought alloys and their products strongly depend on the process conditions imposed during almost each fabrication step (i.e. casting, homogenization, hot and cold rolling and annealing). It is specific to aluminum as compared to other materials, that already very early process stages take effect on the final properties. Therefore, the control and optimization of properties requires sound knowledge of the underlying mechanisms and the sometimes complex interactions between metallurgical and processing parameters. These are well developed in plant experience, usually based on trial and error. But the implementation of new alloys and processing routes involves extensive testing, which is very costly and time consuming. For these reasons, research in the area of what is termed today Integrated Computational Materials Engineering (ICME) has been conducted in the Aluminum industry since the late 1990s (e.g.[1]) at that time termed Through Process Modeling (TPM). In 2000, three coordinated projects, funded by the European Union as VIR* were initiated to develop and apply new simulation tools and methods to integrate physically based models to the main wrought alloys and their fabrication routes. The result was a “TPM” exercise that proved the

validity of the different material and microstructure models, integrated into process models of industrial practices [2].
Meanwhile, models are well advanced and increased computation power allows for applications in many areas. Thus TPM is often not only used for designing new alloys or novel production technologies or routings but it serves also the analysis of running processes in order to achieve more stable process windows, to allow for tighter tolerances in final properties or to avoid production problems.

Modeling of the Rolling Process Chain

The models being applied in this study are briefly described in the following. RoseRoll [3] (ROSE=Rolling Simulation Environment of Hydro Aluminium) represents a thermo-mechanical code, employed to simulate rolling. It is a dedicated 2D code for fast application on multi-pass hot and cold rolling including inter-pass times. A number of material models are incorporated in a fully coupled mode. These are Strucsim [4] for the modeling of separate structures as they occur in partial recrystallisation situations and 3IVM [5-7] for work hardening and dynamic and static recovery, based on dislocation statistics.
The combined models Strucsim and 3IVM in their original versions accounted for the state of solute and precipitates (microchemistry) by the use of metallo-physical parameters, which were adjusted for a specific alloy. In the extension as described below, they now take as input the amount of solutes as well as the amount and size of particles being formed in previous operations. These must be determined either by measurement or by a microchemical simulation. The numerical model used for this purpose is ClaNG (**C**lassical **N**ucleation and **G**rowth) [8, 9], which considers the processing and the chemistry effects on particle precipitation and dissolution. ClaNG is based on the theory of nucleation and growth of secondary phases and multi-component thermodynamics and is linked to thermodynamic databases, which provide the phase diagram information [10]. The main input to the model is the time/temperature history and the alloy composition, whereby Si, Fe, Mn, Mg, Cu, Cr, Ti can be selected for modeling. For an accurate prediction of the nucleation sites for precipitation, the dislocation density accumulated during the preceding operations, has to be provided.
Furthermore, RoseTem is a FDM based thermal model to simulate coil heating and cooling processes in combination with RoseStat to determine static recovery and recrystallisation during these processes. Furthermore a module RoseWind [11] is available to calculate the mechanics of winding operations of strip to coils. These models run in a decoupled mode. A successive coupled mode is accomplished between all models via standardized interfaces, which enable the exchange of pre-treated materials between the models and allows for a comparative application of different model combinations on the same processes or material state.

Material models for prediction of hardening and softening behavior

The 3IVM+ model (3-Internal-Variable-Model) predicts the flow stress evolution of cell building metals, such as Aluminium and Aluminium-alloys.
The three internal state variables of the model are the mobile dislocation density ρ_m, the immobile dislocation density in cell interiors ρ_i and in cell walls ρ_w. These variables represent the microstructure of the modeled alloy.
In the course of a forming process, dislocations move and a number of interactions with other dislocations, e.g. annihilation, dipole formation, lock formation take place. The corresponding evolution of each type of dislocation density is described by the structure evolution equation:

$$\dot{\rho}_{m,i,w} = \dot{\rho}^{+}_{m,i,w} - \dot{\rho}^{-}_{m,i,w} \qquad (1)$$

where $\dot{\rho}^+$ and $\dot{\rho}^-$ are the dislocation production and reduction rates, which are influenced by temperature, strain rate and the microstructure itself.
In order to calculate the macroscopic flow stress k_f, which is required to achieve the imposed strain rate $\dot{\varepsilon}$ for a given temperature T and microstructure, the kinetic equation of state (a partial derivative of the Orowan equation) is applied:

$$\dot{\gamma} = \dot{\varepsilon} \cdot \overline{M} = \rho_m \cdot b \cdot \upsilon(\tau_{eff}, T) \tag{2}$$

where $\dot{\gamma}$ is the shear rate, $\overline{M}$ the average Taylor factor, b the magnitude of the Burgers vector; υ is the average dislocation velocity, which is a function of effective stress τ_{eff} and temperature T.
The shear stress in the cell interiors and cell walls, which enables dislocation slip, is the sum of the passing stress of dislocations and the increment of shear stress coming from alloy chemistry τ_{chem}:

$$\tau_{i,w} = \alpha \cdot G \cdot b \cdot \sqrt{\rho_{i,w} + \rho_m} + \tau_{chem} \tag{3}$$

where α is the geometric constant, G the shear modulus, $\tau_{chem} = \tau_p + \tau_{sol}$; τ_p is the increment of shear stress from particles [12] and τ_{sol} the increment of shear stress from solutes [7]. The macroscopic flow stress can be then calculated using the following equation:

$$k_f = \overline{M}(f_i \cdot \tau_i + f_w \cdot \tau_w) \tag{4}$$

where f_i and f_w are the volume fractions of the cell interiors and cell walls, respectively.
To model the static recrystallisation, a dislocation density based recrystallisation model is combined with 3IVM. This approach enables an accurate consideration of the recovery effect on recrystallisation nucleation and nuclei growth. The driving force for static recrystallisation arises from the total dislocation density, which is composed of the dislocation density fractions in the cell interiors and cell walls, being predicted by 3IVM.
The velocity of the growth (=grain boundary velocity υ_{GB}) is calculated using the following simplified expression:

$$\upsilon_{GB} = m \cdot p \tag{5}$$

where m is the grain boundary mobility and p is the driving force for grain boundary motion. In the presence of dispersoids and solutes the driving force p is strongly affected by the Zener drag p_{Zener} and the solute drag p_{Sol}:

$$p = p_{RX} - p_{Zener} - p_{sol} \tag{6}$$

In the model, Zener drag is considered for the two most common particle types in the alloy. Solute drag is calculated using the approach, proposed by Lücke and Detert [13].
Finally, the recrystallized fraction f_{RX} can be calculated using the "up-dated" grain boundary velocity values, by integrating the function for the recrystallisation rate:

$$\frac{df_{RX}}{dt} = (1 - f_{RX}) \cdot 4 \cdot \pi \cdot N_0 \cdot r^2 \cdot \upsilon_{GB} \tag{7}$$

where $(1-f_{RX})$ is the fraction of the unrecrystallized microstructure, N_0 the density of nuclei and r the recrystallized grain radius.

Simulation of creep

A special attention in this study is devoted to the effect of creep on the coil quality, whereby the focus has been put on the sheet flatness. For creep modelling a phenomenological description of creep rate $\dot{\varepsilon}$ as a function of the internal stress σ and temperature T is commonly used: